KLOE note # 171
December 1998

Equipment and procedure for stringing the KLOE drift chamber

G. Bencivenni, P. Campana, G. Catitti, S. Dell'Agnello, U. Denni, M.A. Frani, G. Finocchiaro, S. Moccia
Laboratori Nazionali di Frascati dell'INFN, Frascati, Italy

R. Assiro, V. Elia, G. Fiore, V. Golovatyuk, F. Grancagnolo
Dipartimento di Fisica dell'Università di Lecce and INFN Lecce, Lecce, Italy

F. Bronzini, A. Pelosi
Dipartimento di Fisica dell'Università "La Sapienza" and INFN Roma I, Roma, Italy

P. Valente
Dipartimento di Fisica dell'Università di Roma "Tor Vergata" and INFN Roma II, Roma, Italy

Abstract

The KLOE tracking detector, with its 4 m diameter, 3.3 m length and 52,140 wires, is the biggest drift chamber ever built. The stringing of this impressive number of wires with the requested quality characteristics has been a gigantic work, successfully completed in 11 months, not far from the expected schedule. A dedicated semi-automatic facility was developed to perform the stringing. The robotic system together with the stringing procedure is described here. The hardware and the software aspects of the system, the optimization of the critical parameters of the stringing operation, and the quality checks performed on the strung wires are described.

1 Introduction

The KLOE Drift Chamber is a detector unconventional under many aspects; its main characteristics are dictated by the physics demands of the experiment [1]:

- a large and homogeneous volume for the isotropic decays of the K_{L};
- a good momentum resolution for charged particles of momenta as low as 50 MeV/c;
- high transparency to minimise multiple scattering and conversion of low energy photons (down to 20 MeV).

These demands led to the choice of an impressively big single-cell drift chamber: 4 m diameter, $\simeq$ 3.3 m length; the mechanical structure is entirely made in carbon fiber. The wire materials are 25 μm gold-plated tungsten for sense wires and 80 μm silver-plated aluminum for field wires. The two carbon fiber composite end-plates are held apart by 12 carbon fiber struts, which also provide mechanical rigidity. The chamber is closed by 12 carbon fiber honeycomb external panels and an inner 700 μm aluminated carbon fiber cylinder. The total material thickness including cables and low mass electronics is less than 0.1 X_0 [1)].

An all stereo wires configuration was chosen for uniform filling of the chamber: the stereo angles range from 60 to 150 mrad in order to have constant radial drop. The 12,582 cells are approximately square and are arranged in 58 layers – 12 inner layers of $2{\times}2/3\pi$ cm^2 size and 46 outer layers of $3\times\ \pi$ cm^2 size – with a field to sense ratio of 3:1. Including the first and last layers of guard wires to correctly shape the electric field, there is a grand total of 52,140 wires arranged on 119 layers.

The nominal tension of the wires was chosen in order to have for the wire sagitta a uniform value of 250 μm throughout the chamber. Since the total load due to the tension of the wires amounts to 3.5 tons on each carbon fiber end-plate, the latter would undergo a non-negligible deformation, of the order of 3 mm. Such a deformation would also correspond to a significant increase of sagittae and of sagittae disuniformity, so that the effect has to be corrected for. A carbon fiber ring surrounds the external flange of each end-plate in order to allow the application of a radial force to the end-plates themselves, through a series of screws (see fig. 1): the end-plates, acting as membranes being radially pulled, recover their deformation [2] (details on the structure of the chamber and its construction can be found in [3]).

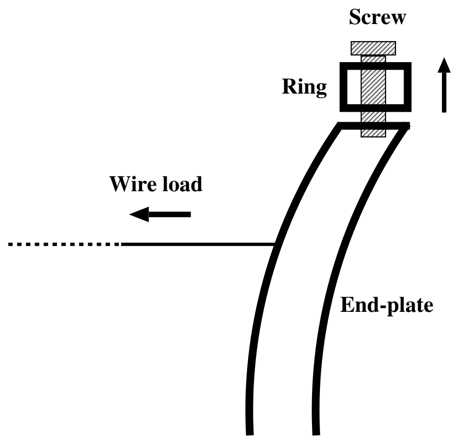

Figure 1: Schematic view of end-plates tensioning ring.

[1)] Using a 90% He - 10% iC_4H_{10} gas mixture the radiation length inside the chamber including the wires is about 900 m.

An additional effect for aluminum wires is the well known phenomenon of creep, that is non-elastic deformation under a load [4]. The nominal tensions of the wires was therefore re-calculated in order to get uniform sagittae at the end of the stringing, taking into account all these effects and the deformation recovery due to periodic tensioning of the external ring: this strategy is fully described in [5].

The wires are fixed to the end-plates with feed-throughs, like the one depicted in fig. 2: a conical plastic bushing (maximum diameter 3.00 mm) is molded round a metallic pin (diameter 1.00 mm). The wire is inserted into the feed-through and fixed by a crimping performed by pneumatic pliers; then the feed-through is inserted into the hole in the end-plate.

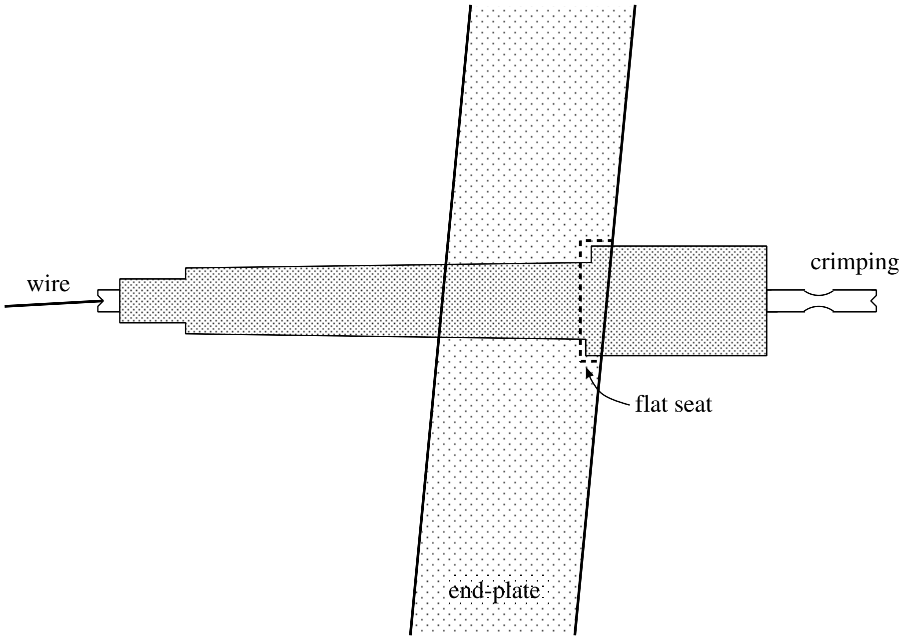

Figure 2: Schematic view of the feed-through fitting inside the hole in the end-plate (transverse section). The conical plastic bushing (shaded) is molded round the metallic pin (white).

Quite naturally the stringing proceeded from the innermost layer to the outmost, layer by layer: the procedure is described in detail in section 3 and essentially consisted of three phases:

- wire transport across the chamber end-plates through the correct holes (which means at the correct stereo angle) starting from the $z_{\mathrm{KLOE}} < 0$ end-plate, which we call side *A*, to the opposite end-plate, on side *B* ;
- on side *A*: wire insertion into the feed-through and insertion of the feed-through in the hole in the end-plate, then crimping of the feed-through;
- on side *B*: wire insertion, feed-through insertion, tensioning of the wire at the right mechanical tension and crimping.

Stringing such a detector required the construction of a dedicated, semi-automatic stringing facility: while the rotation of the chamber, the transport of the wire, the positioning of the crimping stations and the crimping of the feed-throughs are performed automatically, some operations as the insertion of the wire inside the feed-through and of the feed-through into the hole are performed manually. All the hardware is described in the following section.

2 Hardware description

The stringing was performed in a clean room, class 1,000 in the area of the chamber and class 10,000 in the surrounding working area, in order to minimise dust on the wires. The temperature of the clean room was kept stable within $\pm$ 1°C, to avoid thermal elongations of the wires.

The stringing system was designed in order to:

- support the chamber structure;
- rotate the chamber to any angle;
- stretch the wires between the holes in the end-plates safely, i.e. pulling the wire with a constant strenght and without touching the wire itself;
- pull the wires at the correct mechanical tension and crimp the feed-throughs.

A schematic overview of the stringing system is shown in fig. 3: the reader can see the end-plate *B*, the system for the rotation of the chamber and the side *B* platform, where one of the two operators worked on the external crimping station: a similar platform and crimping station were on the opposite side *A*, not shown in the picture. On the right, the wire carrying robot and its supporting structure are shown. All elements of this system are described in the following sections.

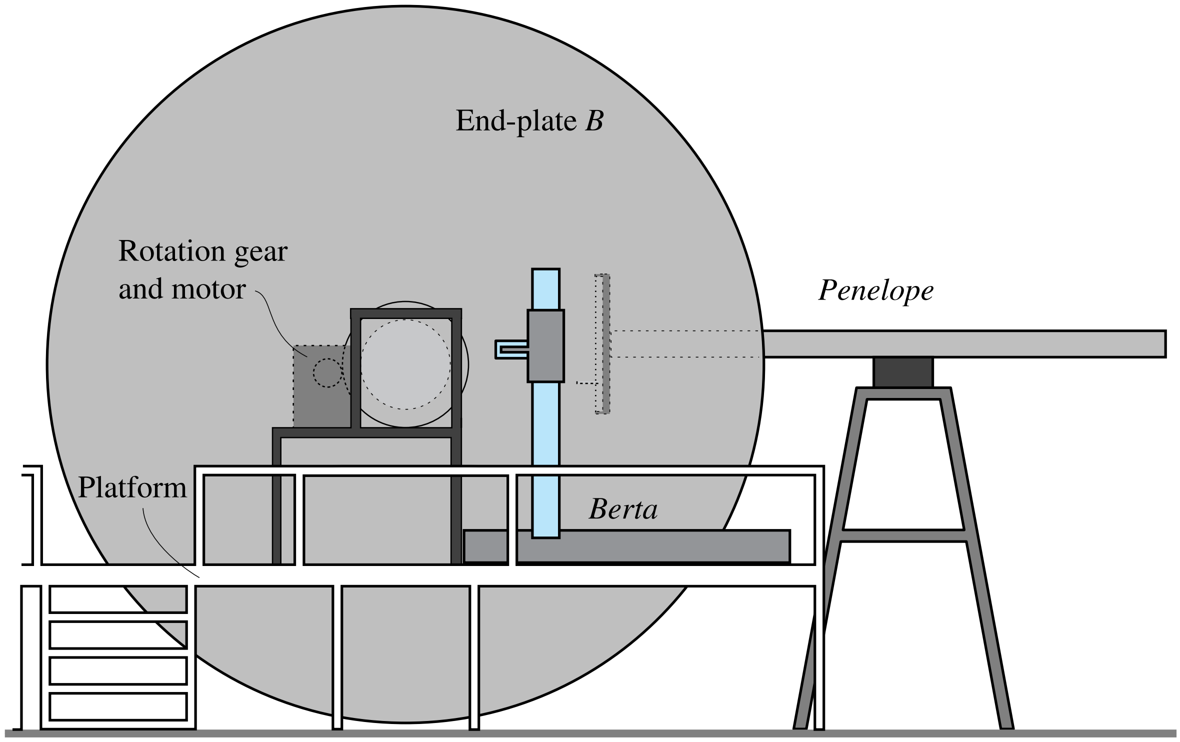

Figure 3: A schematic general view of the stringing system (see text for the definition of names), from side *B*. The rotation system supporting the whole chamber was coupled to the rotation motor through a gear. The platform (in white) where the operator worked on the external crimping station (*Berta* on side *B*) is also shown together with the stairs and safety railings. The wire carrying robot, *Penelope*, is shown partially inserted into the chamber.

2.1 Rotation

The structure was supported by a steel rig, mounted on linear bearings. The two end-plates were coupled to the rig by means of steel supports, fixed to the internal flanges. The supporting rig was coupled with of a gear to a low speed DC motor (see fig. 4).

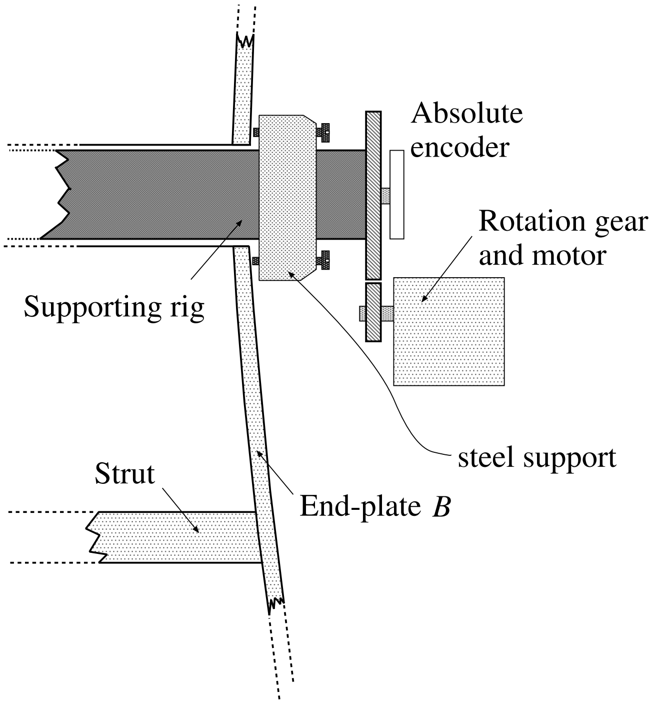

Figure 4: Schematic top section of the chamber supporting system (not to scale).

The rotation of the system was controlled by means of a high precision absolute encoder. The measured position accuracy, dominated by the mechanical couplings, is of the order of 200 μm at the maximum radius of 2 m.

2.2 Wire transport

The wire transport from the end-plate *A* to the end-plate *B* was performed by a three movements robot, called *Penelope*. The three movements are approximately along the x,y and z directions in the KLOE reference system. The *Penelope* main axis was aligned to the chamber axis, i.e. along z. An arm, that we call x arm, could move on the z support along two directions, as shown in fig. 5:

- longitudinally along the main axis: we call this the z movement;
- transversally, towards the inside and outside the chamber (x movement).

An additional vertical arm, equipped with a wire carrying tool moving along the arm itself (y movement), was needed in order to reach all the holes in the end-plates, because of the stereo configuration of the wires (fig. 6).

During the stringing, the rotation of the chamber was limited by the presence of the x arm between the struts; this means that some holes had to be reached from "behind the strut", i.e. with a configuration as the one depicted in fig. 5: the x arm was inserted between a pair of struts, at the x depth necessary to reach the current layer, and the chamber was rotated to the maximum angle allowed by the presence of the x arm of the robot (with some safety margin). In this position the y arm, which in a lateral view is behind the strut, allows the wire carrying tool to reach the right hole with the y movement. The length of the vertical arm was determined taking into account the maximum wire stereo angle (the one at the largest radius) and the mechanical dimensions of the *Penelope* x arm, in order to reach all the holes in the end-plates.

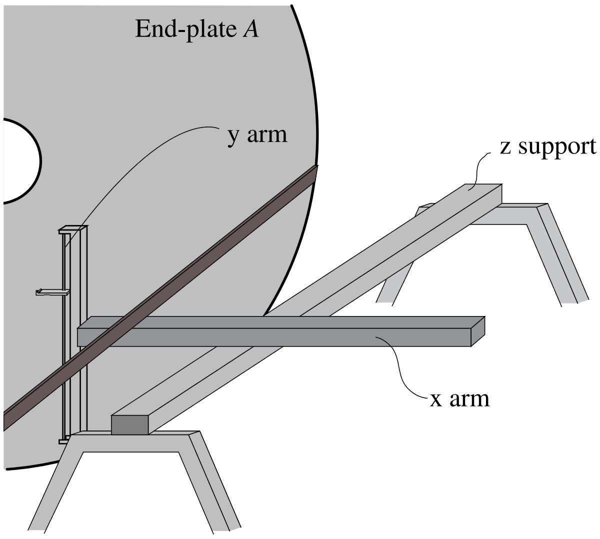

Figure 5: Schematic view of the chamber and of the wire transport robot in the stringing configuration with the y arm "behind the strut" (see text).

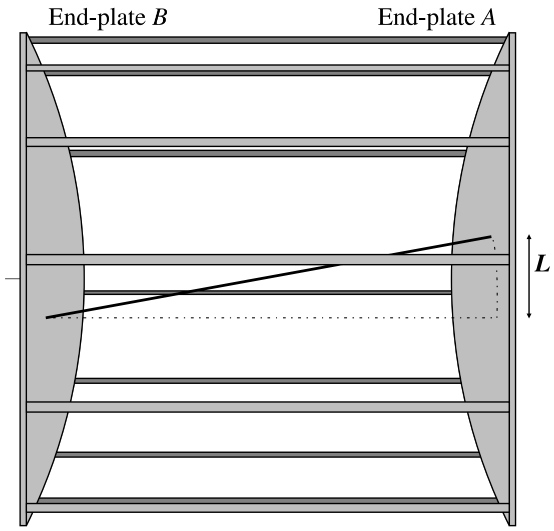

Figure 6: Schematic side view of the chamber: the wire transport robot needs a vertical movement in order to reach all the holes, due to the stereo angle and the presence of the 12 struts (see text).

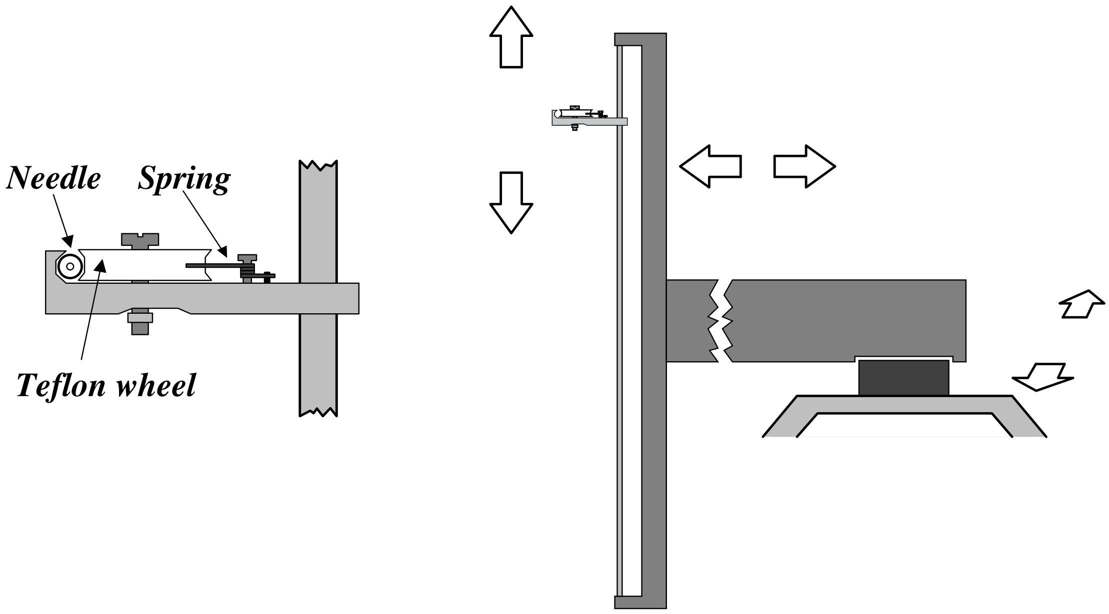

Figure 7: Right: schematic view of the *Penelope* robot movements with the fixed arm (y movement); left: detail of the wire carrying extension or "nose".

The 105 most internal layers were strung with this fixed y axis, mounted at the end of the x arm (fig. 7). For the outer layers, the available space between the already strung wires and the struts was so small that the y arm could not be inserted "behind the strut". A smaller, rotating arm (ϕ movement, see fig. 8), was designed and built in order to complete the stringing.

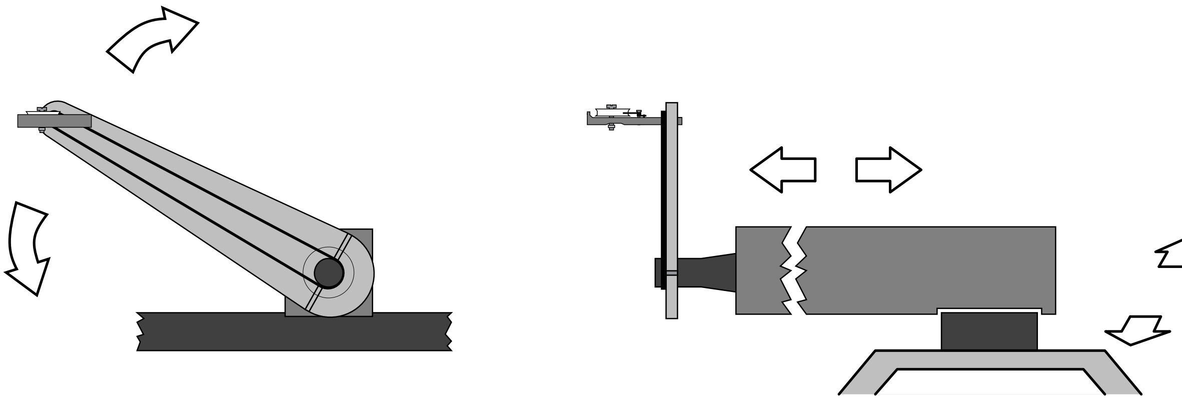

Figure 8: Schematic view of the *Penelope* robot movements with the rotating arm (ϕ movement).

The wire, inserted inside a special steel needle, was manually supplied to a needle-carrying extension of the arm, called "nose", which hold the needle by a teflon disk pushed by a small spring (see fig. 7). All movements were achieved by step motors and controlled by incremental encoders.

In order to reach and string all the layers of the chamber, accessing the end-plates from one side, the *Penelope* "x arm" was more than 2 m long, so that it bendt of a sizeable amount, up to 2 cm at the x depth necessary to string the very first layers of the chamber, under its own weight. A correction depending on the x position of the arm was therefore introduced in the coordinate calculation, using a set of accurate optical measurements of the lowering of the arm (as shown in fig. 9).

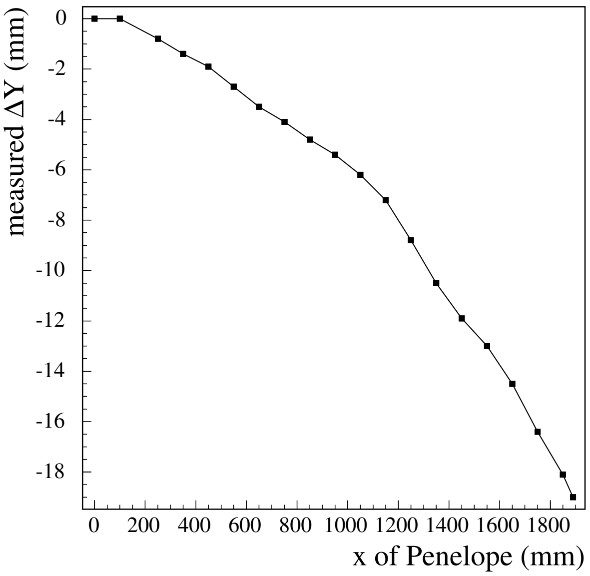

Figure 9: Measured lowering of the *Penelope* arm, due to its own weigth, as a function of $x_{Penelope}$ ($x_{Penelope} = x_{offset} - x$).

Taking into account this correction, the positioning of the "nose" was made accurate at the level of 500 μm. This nicely fit our requirements, deriving from the diameter of the 3 mm holes in the end-plates.

2.3 Wire tensioning and crimping

The crimping of the feed-throughs was performed by means of pneumatic pliers mounted on two external stations:

– *Arianna*, the side *A* crimping station, togheter with the wire supply system;
– *Berta*, the side *B* crimping station, togheter with the wire tensioning system;

Both stations had three axes movements (see fig. 10) spanning a portion of the end-plates wide enough to cover the whole range of stereo angles. The axes were moved by step motors coupled to incremental encoders. The overall positioning accuracy was $\simeq$ 200 μm.

The crimping parameters, such as the shape of the pliers' jaws, the crimp depth and length, were carefully optimised (see details in [6]). Since the crimping area is longitudinally $\approx$ 1 mm out of a 5 mm pin length (see fig. 2), the positioning of the pliers must be accurate, better than 0.5 mm, in order to have a good crimp and avoid damages to the wire or to the feed-through.

The distance between the metallic pin (which is to be crimped) and the crimping machine was not constant so that the position of the crimping area showed variations up to 2 mm from its nominal value. This was both due to small shape irregularities of the end-plates and the not perfect coupling between the feed-throughs and the end-plates holes.

To overcome this problem, the distance of the crimping pliers was adjusted by software, reading a depth-gauge, fixed to the z axis, which gave a feed-back to the z axis approach to the

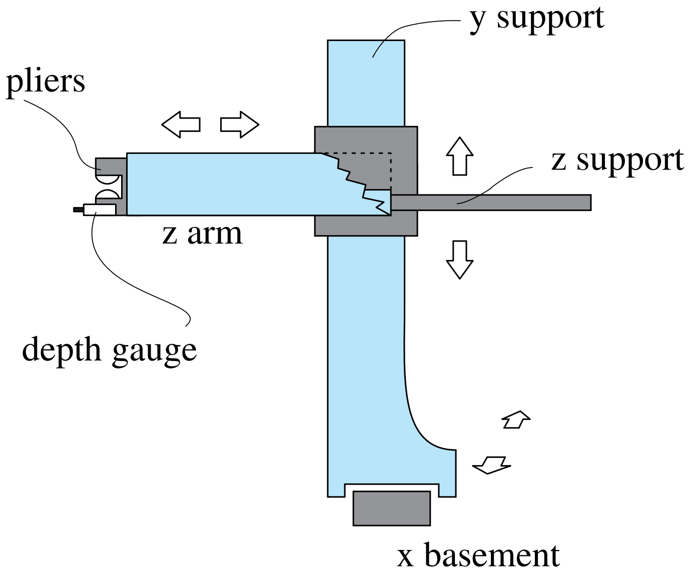

Figure 10: Schematic side view of an external station.

end-plate. The accuracy of this depth-gauge correction had two limiting factors: the irregularities of the thin ($\sim$ 30 μm) copper foil glued onto the two carbon fiber end-plates to provide a ground, and by the dead-time introduced by the computer to read out the analog output of the depth-gauge. The required accuracy was achieved by slowing down the z movement while approching the end-plate.

The wires must be pulled at the right mechanical tension, calculated following the criteria explained in [5]. The tensioning was done by means of a rotating fluted wheel driven by a step motor and coupled to a torquemeter (see fig. 11).

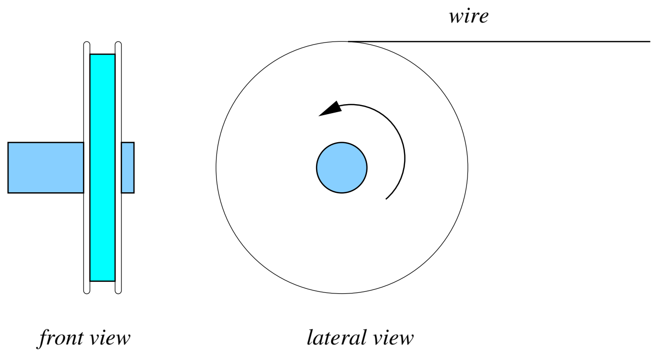

Figure 11: Schematic view of the wire tensioning device (torquemeter).

The instantaneous tangential force on the wheel was measured by strain gauges, whose output current is proportional to the torque on the wheel axis. This current is fed into an ADC channel read out by the computer. After a static calibration with a set of known weights, the torquemeter can read the tangential force on the wheel, while pulling the wire. The calibration was periodically repeated in order not to spoil the accuracy of the tool, moreover the electronic zero offset was subtracted with an automatic software procedure (see the window of the *stringing program* at lower left side of fig. 14). The wire was pulled in two phases:

- a fast rotation phase, during which the loose wire was pulled until it gained a small tension;
- then a very slow rotation phase, during which the wheel was moved in small steps in order to pull the wire at the requested tension with the highest possible accuracy.

The overall accuracy of the tensioning procedure can be estimated by comparing the measured values of the tension (the measurement of the mechanical tension of the wires was performed at the end of the stringing of each layer) with the nominal ones, and was better than 5% (fig. 12).

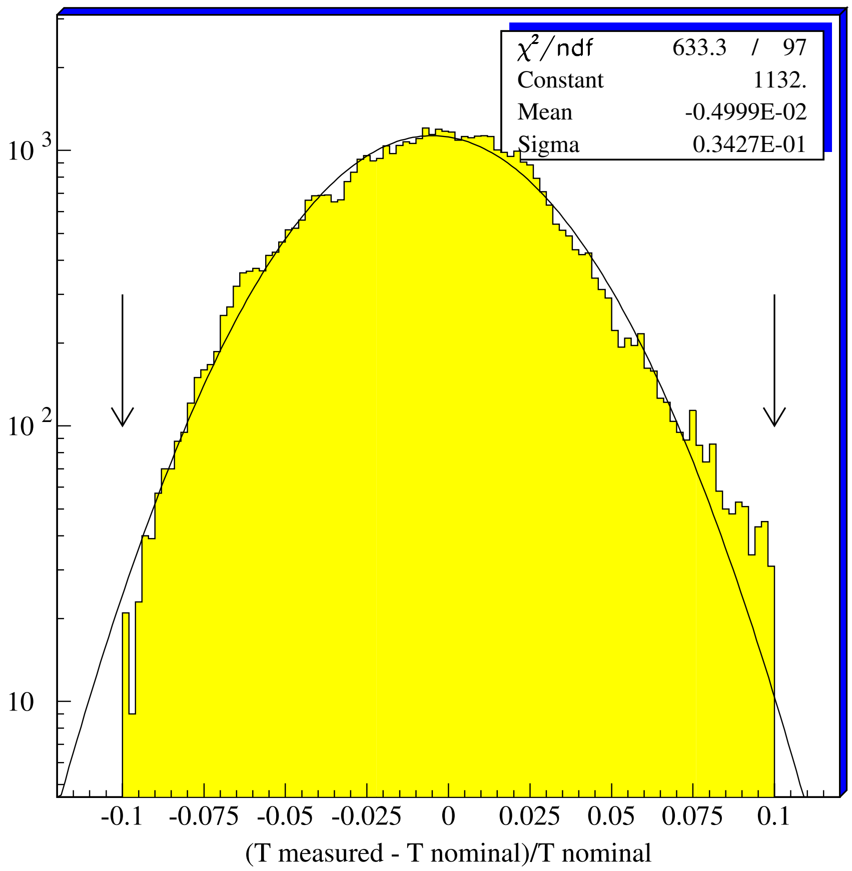

Figure 12: Difference between the measured and nominal tension of all the wires after stringing. Wires with a relative difference above 10% were immediately replaced.

2.4 Control system

The movements of the axes of all robots, *Penelope*, *Arianna* and *Berta*, were achieved by means of step motors, driven by commercial programmable servo-mechanism controllers, S&H *Michelangelo*™ three axes controllers. The rotation DC motor was also driven by a dedicated *Michelangelo*™. The *Michelangelo*™'s are controlled via serial ports by a unique *stringing program*, written using the National Instruments *LabView*™ development environment on a Apple *Macintosh*™ Quadra 950 computer.

The incremental encoders were read out by the controllers and used as a feed-back for software coordinate correction, in order to achieve the positioning precision quoted above. The *Michelangelo*™'s also provide warnings and alarms for anomalous situations handling: dedicated digital lines were connected to emergency stop buttons and end-run switches provided a master alarm signal, which caused the interruption of all movements and started an emergency procedure to be handled by the operator of the *stringing program*, called "stringing expert".

All the different phases of the stringing procedure (section 3) were synchronized by the *stringing program*: the two stringing operators interact with the program using a console, one on either side, with warning lights and buttons. Operators pressed the appropriate button when ready for the next operation, and were acquainted by the switching of the warning lights. The consoles' buttons and lights were controlled by the program via digital ports.

The acquisition of the torquemeter and of the depth gauges reading used for the correction of the z coordinate of the crimping stations (see 2.3), was performed by an ADC board on the *stringing computer*.

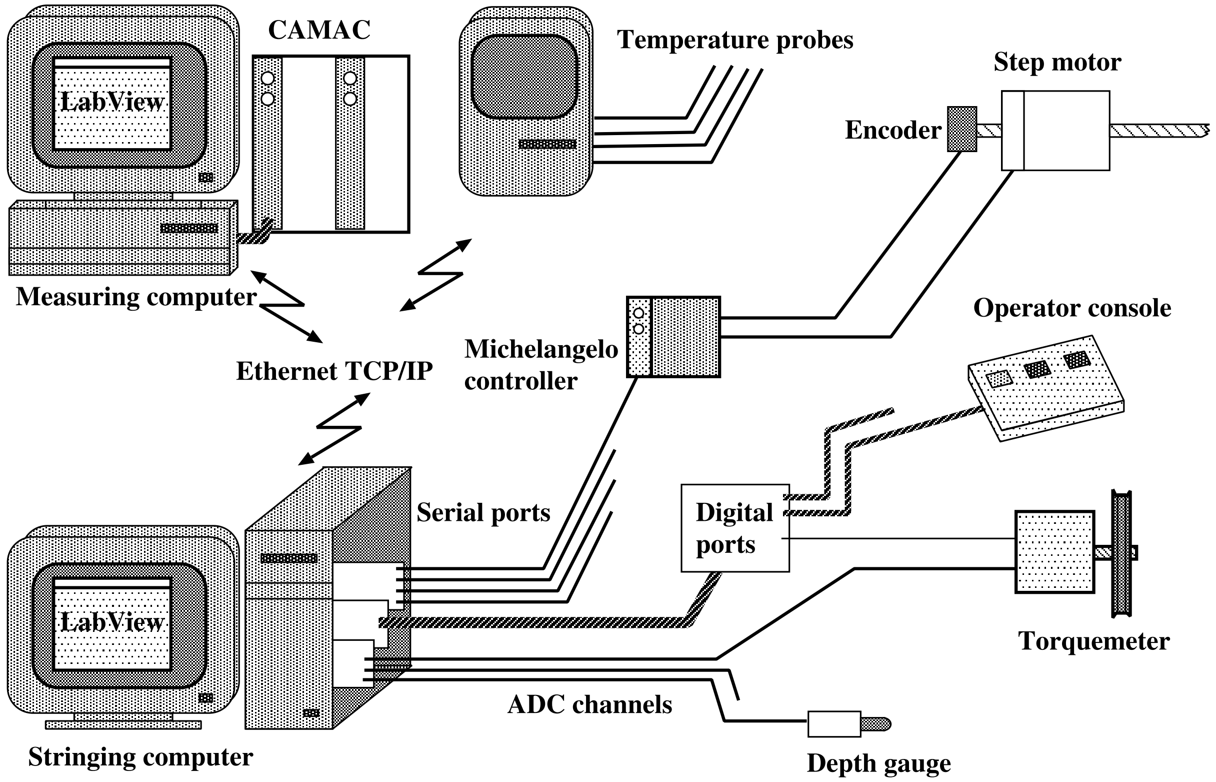

Figure 13: Scheme of the stringing control system.

In figure 13 a scheme of the control system is shown: the controllers of the robots and ancillary systems, such as consoles, torquemeter and depth gauges and digital lines are shown.

The mechanical wire tension measuring system (which is described elsewhere [7]) was controlled by a dedicated computer, and could be run during the stringing operation. This separate process had to be synchronized with the rotation of the chamber. The measuring system must in fact know the present rotation angle of the chamber in order to determine the wire being tested. The *stringing program* handled all this, communicating via TCP/IP on the Ethernet network with the measuring system computer: the measurement triggered by the *stringing program* was sent back to the stringing computer and written to the general database with all the strung wires data.

Finally, the *stringing program* constantly had a connection to a small computer controlling the temperature and humidity, using several probes in different places of the clean room. In fig. 14 a screen capture of the panels of the stringing program is shown. On the top left corner of the picture the main panel shows the information about the current wire being strung. This picture was taken on the very last strung wire, on layer 119: an additional panel is warning the "stringing expert" that wire has to be transported manually since the holes on the last layer can not be reached by the robot. The main panel also shows the status of the communication with the measuring computer. On the bottom left corner the panel displaying the offset measurement of the torquemeter is shown: before pulling the wire the system automatically subtracted the offset of the ADC reading of the torquemeter signal, in order to achieve the requested accuracy on the wire mechanical tension. On the bottom right corner a panel shows the torquemeter instantaneous reading of the wire mechanical tension while pulling. In the picture the display of the tensioning of the last five wires is visible: the steep slope corresponds to the first, faster pulling phase, while the mild one to the slow, more accurate, pulling phase.

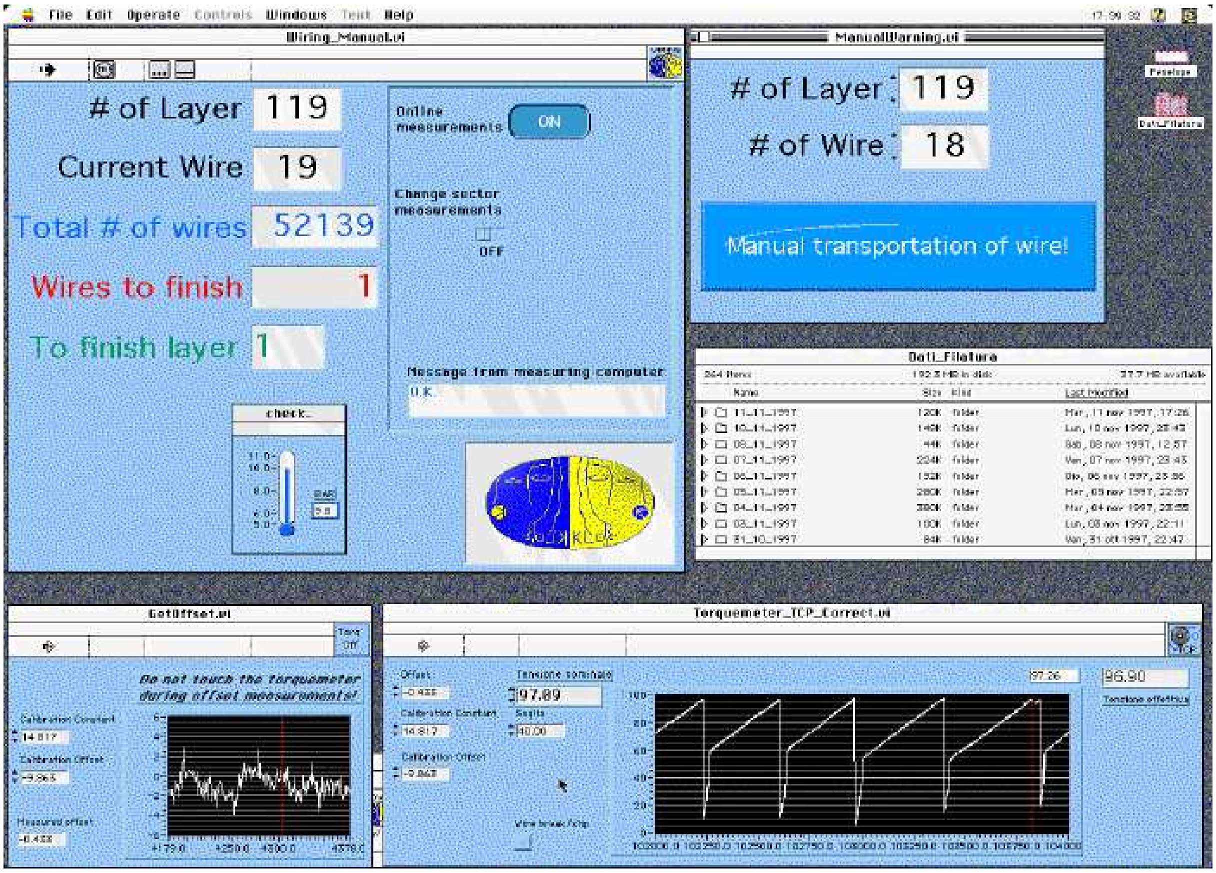

Figure 14: Screen capture of the *stringing program* panels (see text).

3 Stringing procedure

The stringing procedure was optimized in order to have minimum time needed to string a wire, while guaranteeing that the wire itself was safely handled (actually with the adopted solution the portion of the wire effectively stretched between the end-plates was never touched at all by the operators). The operations on the two end-plates proceeded almost in parallel, except for those which needed the completion of a phase on the other end-plate: for example the wire could not be pulled before being crimped on the other side.

On side *A* the operator had to:

- insert the wire into the needle, checking the wire type light, and wait until the green button is on (the previous pin has been crimped and the crimp has been checked);
- insert the needle into the hole and push it into the “nose”, then push the green button (*Penelope* starts moving towards plate *B*);
- wait until the red light switches off (when side *B* has received the wire and has pushed the green button), then block the wire and cut it (while waiting the operator also prepares a new needle with the next wire);
- push the green button again if everything is OK or push the red one if the wire is lost (for example, if the needle slipped out of the nose, or the wire broke);
- insert the wire into the feed-through and insert the feed-through into the hole;
- push the green button and, after station movement and crimp, check the crimp;
- push the green button if everything is OK (side *B* can now tension the wire and crimp), or push the red one otherwise;
- start with the new wire.

On side *B*:

- wait until the green and red buttons are on, then take the needle from the hole and block the wire;
- push the green button if OK, or push the red one if the wire is lost or broken (*Penelope* starts moving back towards plate *A*, waiting for next wire);
- take the wire from the needle and insert it into the feed-through, then insert the feed-through into the hole;
- push the green button (side *A* can now cut the wire);
- block the wire on the torquemeter and wait until the green button is on again (side *A* has crimped);
- push the green button and, after station movement and crimp, check the crimp;
- push the green button if everything is OK, or push the red one otherwise.
- start with the new wire;

With this sequence, the wire transport between the two end-plates and the return of the *Penelope* robot occurs when the two operators are busy with some other operation:

- completion of the previous wire on side *B* and preparation of the needle on side *A*, during transport;
- crimping operations on both sides, during the return of *Penelope*;

In this way no dead time is introduced.

4 Operative experience

The most critical operations during the stringing procedure were found to be:

- the quality checks performed on the strung wires, after completion of each layer: both for the time necessary to perform the checks and for the number of wires rejected and to be replaced;
- the crimping quality, in particular the depth of the crimping had to be kept continuosly under control, since a difference from the nominal parameters of the crimping tools could

result in either wire slipping, in case of reduced pressure, or wire breaking, in case of over-pressure;
- the skill of the two operators on the end-plates and their periodical turn-over – every three months – and consequentely their learning period;
- the time necessary to string a wire, both instanteous and averaged over the period of a shift of the operators, including interruptions due to “micro-problems”.
- the effect of the deformation of the end-plates and of the periodical operation of deformation recovery [2]: the mechanical wire tensions after stringing and after each tensioning of the external ring, had to be monitored in order to achieve uniform sagittae at the end of the stringing.

4.1 Quality checks

Two kinds of quality checks were performed on all wires upon completion of a layer or, partially in parallel with the stringing:

- measurement of the current drawn by the tungsten wires: a wire was kept at a voltage of 1 kV for $\approx$ 1 minute, and rejected if it drew more than 1 μA in air. For this measurement a very critical parameter is the air relative humidity: the current grows exponentially with the humidity content, which was kept by the feed-back system of the clean room at a value of 50%.
- mechanical wire tension measurement for all the wires [7]: a wire was rejected when the relative difference between the nominal and measured tension was more than 10%.

The procedure of removal and replacement of rejected wire is significantly slower than normal stringing, so that the percentage of bad wires had to be kept small. The percentage of rejected and replaced wires at the end of the stringing (without taking into account wires broken after a while) was $\sim$ 1%.

4.2 Crimping quality

The crimping size, i.e. the diameter of the crimped pin as shown in fig. 15, had to be kept in the range 0.5$\div$0.6 mm in order to have a reliable crimping for both tungsten and aluminum wires: a smaller crimping size can produce wire breaking, a bigger crimping size can result in wire slipping [6].

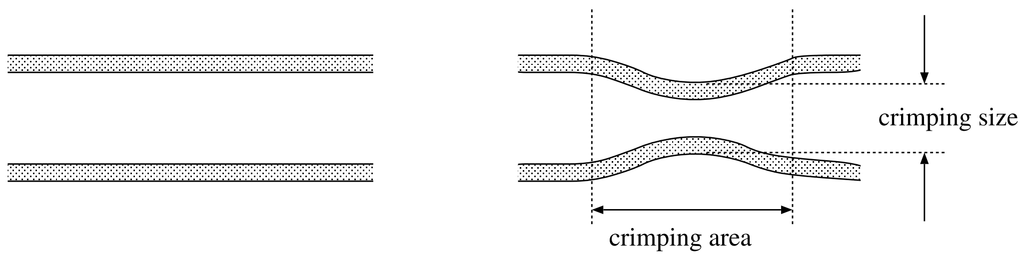

Figure 15: Schematic view of the metallic pin before (left) and after crimping (right). The crimping area and the crimping size definition are also shown.

The crimping size is a decreasing function of the pressure in the pneumantic crimping tools [6], but can also be affected by mechanical breakdowns of the pliers: even if the crimping size was continuosly checked, a set of wires were crimped too strongly by one of the crimping tools.

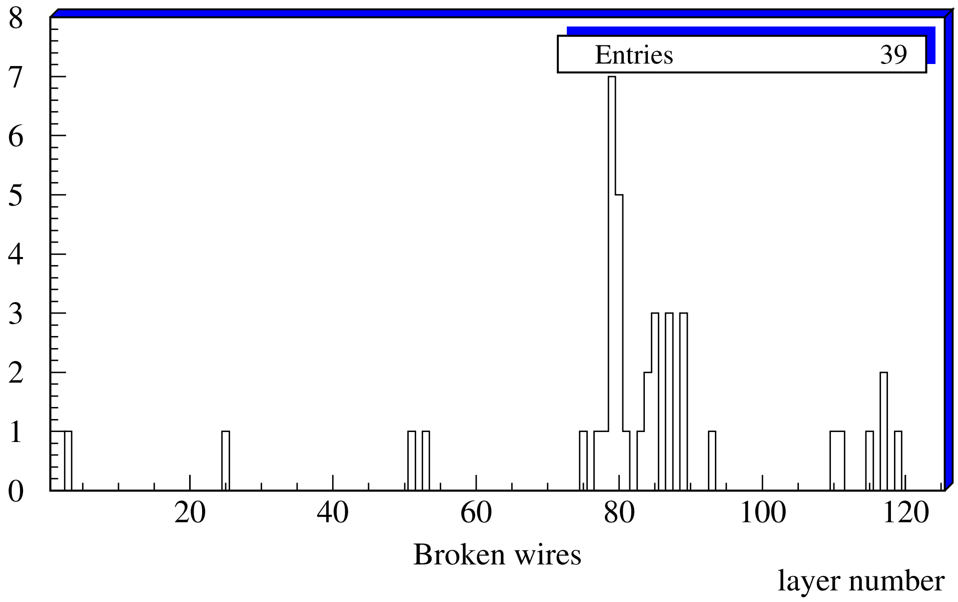

Figure 16: Number of wires broken after stringing.

This was in correspondance of the stringing of layers 78÷85. This is apparent from the peak in the distribution of broken wires at the end of stringing shown in fig. 16.

The replacement of wires in the completely strung chamber has been another challenging work that has been successfully completed and is described elsewhere [8].

4.3 Stringing speed

Even if the foreseen time needed to string a wire was extimated to be approximately 2 minutes, the system soon demostrated that skilled operators could safely complete a wire in 1.5 minutes. The stringing shifts covered 17 out of 24 hours with three alternating crews of two operators on the end-plates and a shift supervisor, who controlled the *stringing program* and all the automatic or semi-automatic systems. The 7 night hours were used for system upgrades and debug, or for additional quality check measurements. Some dead time was introduced at the end of the stringing of each layer, for the measurements on the part of wires which were not checked on-line.

Many other factors have to be taken into account in the time needed to complete, on average, a single wire:

- the skill level of the operators, expecially for what concerns the manual insertion of the wires into the feed-throughs and the interaction with the automatic system through the consoles;
- the long-period efficiency and concentration;
- the occurence of what we called “micro-problems”, such as small interruptions or delay in the stringing procedure due to non-critical errors, which are significant over a long period. One of the most frequent has been the request for human intervention for the recovery

of warning or alarm conditions during the movements of the robot, due to the security devices (hardware and software stops, abnormal conditions in the automatic procedures, etc.). We preferred in fact to be on the safe side, minimising the probability of damaging already strung wires, at the price of slowing down the procedures to recover “emergency” situation. For the same reason, the threshold to define an “emergency” situation was on purpore kept low.

The completion of the stringing of the 52,140 wires of the KLOE drift chamber in less than one year has then to be regarded as a big success. In fig. 17 the number of wires strung as a function

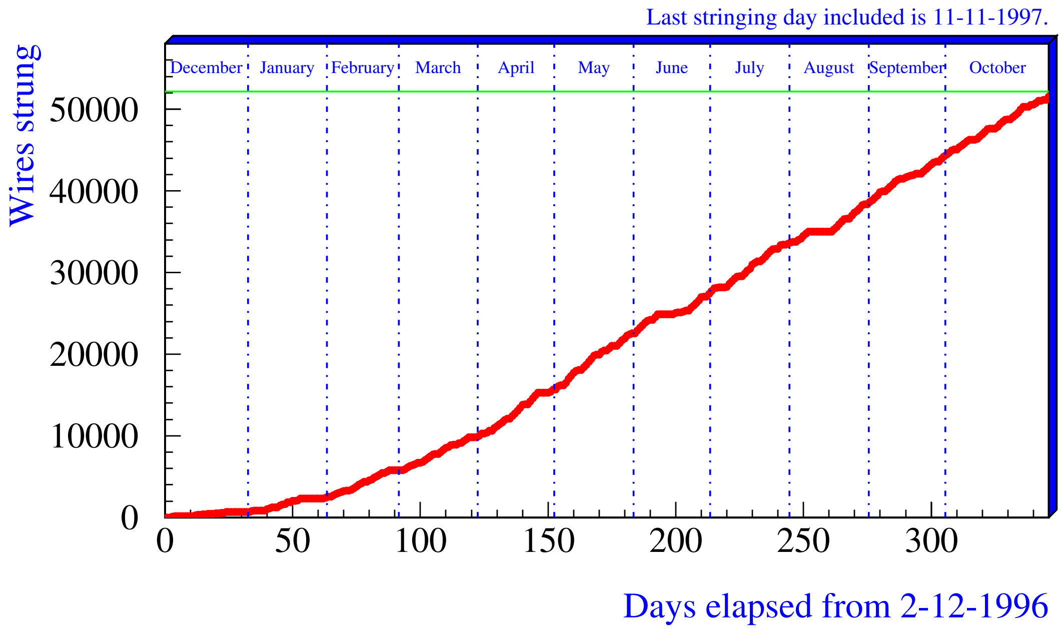

Figure 17: Number of wires strung as a function of the elapsed time. The first 50 days show a low number of wires/day due to the difficult access to the first, inner layers. The larger slope of 180 wires/day from april 1997 ($\sim$ day 150) corresponds to one additional stringing crew.

of the stringing time is shown: the lower speed in the first 150 days was due to reduced shifts (two instead of three crews before april 1997). The low number of wires/day in the first 50 days was due to the reduced access to the first, inner, layers. The learning curve of the operators is not evident, but it can be noticed together with the small plateau’s due to “technical stops”, i.e. the interruption of the stringing for the monitoring of the already strung layers and the periodical tensioning of the end-plates for deformations recovery, as well as the turn-over of the operators crew.

4.4 Sagittae and deformation recovery

Many time dependent effects contribute to the final values of the mechanical wire tension such as the periodic deformation recoveries or the creep effect (on aluminum wires only), so that the time evolution of sagittae could be very complicated, and the final sagittae can be much different from the ’stringing time’ values. A set of reference wires – both aluminum and tungsten wires – at different position on the end-plates and at different radii (i.e. on different layers) were periodically monitored. In fig. 18 the values of the sagittae at the end of the stringing are shown.

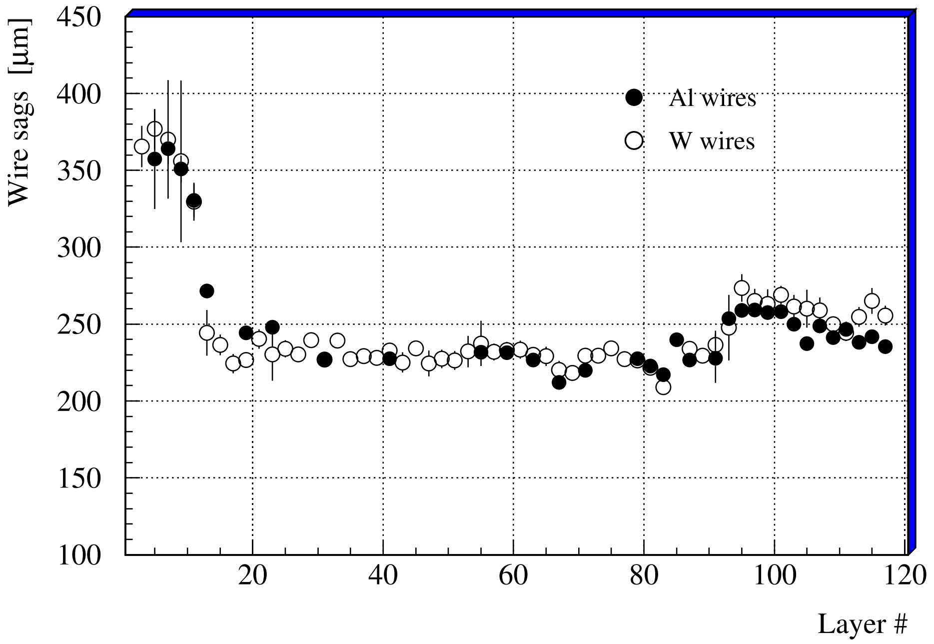

Figure 18: The final values of the sagittae in the KLOE drift chamber. Even if the sagittae were measured immediately after each layer completion, only the values of the reference set of wires at the end of the stringing are reported: since many time dependent effects contribute (periodic deformation recovery, creep, etc.), the time evolution of sagittae can be very complicated, and the final sagittae can be much different from the 'stringing time' values.

The sagittae are effectively very close to the nominal value of 250 μm, while no strong dependance on the radius (i.e. layer number) is observed, excluding the first 12 layers. This is due to the type of bonding connecting the supporting rig and the rotation system to end-plates through the steel flanges shown in fig. 4.

While the first 12 layers were strung the bonding system did not allow the movement of the end-plates; then after the stringing of layer 13 the end-plates deformed under the load of the strung wires and the tension of these wires decreased. Even if it has been partially recovered by the successive tensionings of the end-plates, the final sagittae of these wires are larger, up to 350 μm.

5 Conclusions

The chamber at the end of the stringing is shown in fig. 19. For the first time such a large drift chamber was entirely strung with a robotized system. The construction of the chamber required a huge amount of both hardware and software work and know how on different fields such as mechanics, electronics and software programming.

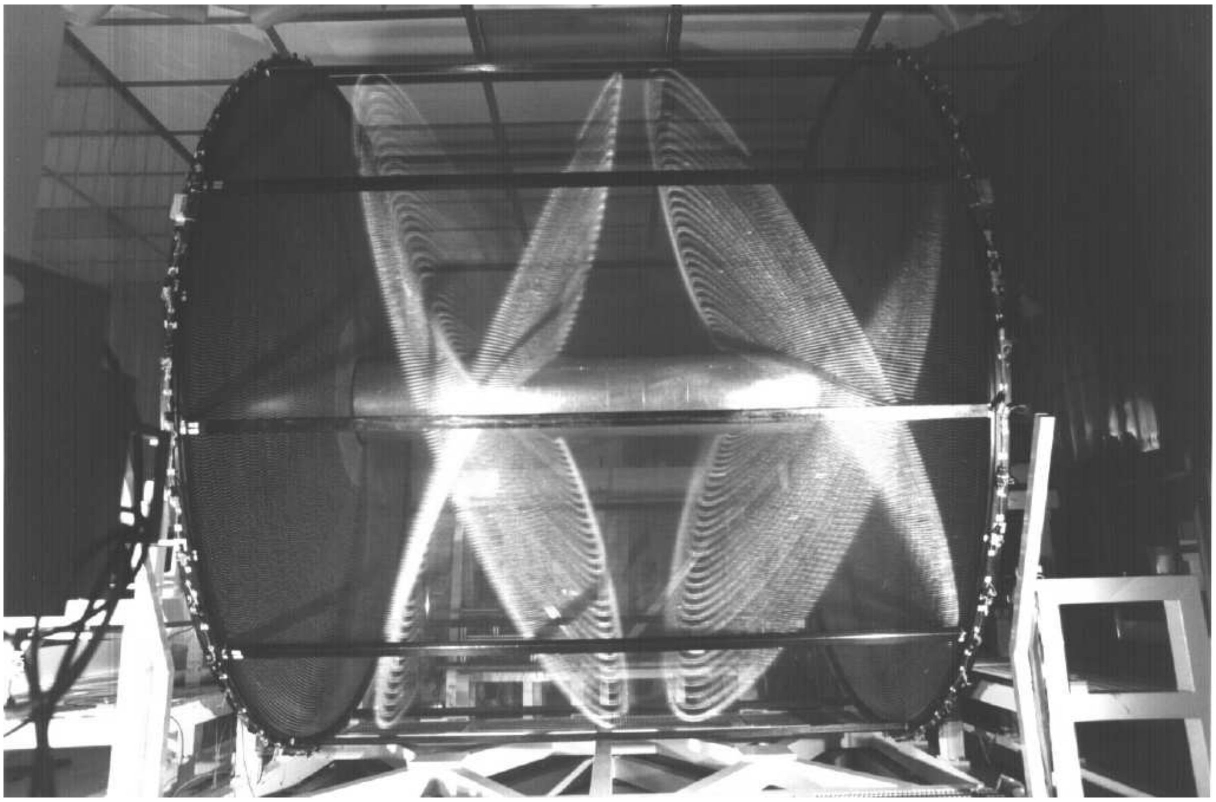

Figure 19: Photograph of the strung KLOE Drift Chamber. The light rings are created by the reflection of light on wires of opposite stereo angle.

Many studies had been preliminary performed, such as the study of the mechanical behaviour of the end-plates under the wires load, the study of the wires characteristics, the design of the feed-throughs and the optimization of the crimping.

Several innovative control systems were successfully implemented, such as the end-plate deformation recovery system or the wire tension measurement device, which allowed a continous monitoring of the wire sagittae.

6 Acknowledgements

We would like to acknowledge the KLOE drift chamber group members who carried on the stringing operations alternating with some of us in 6 hours shifts as “stringing experts”: A. Calcaterra, R. de Sangro, C. Forti, L. Passalacqua, V. Patera, L. Pontecorvo, D. Vettoretti.

We also gratefully acknoledge the technicians who helped us for the construction of the system: G. Bisogni, A. Ceccarelli, A. De Paolis, A. Di Virgilio, G. Ferretti, E. Iacuessa, L. Iannotti, U. Martini, V. Martynov, A. Olivieri, C. Pinto, X. Qing, K. Stroutchkov, L. Wang, S. Zheng.

References

[1] The KLOE Drift Chamber Group, *The KLOE Central Drift Chamber. Addendum to the Technical Proposal*, LNF-94/028(IR) (1994).

[2] S. Moccia, *Design of the KLOE Drift Chamber end-plates*, KLOE note 169, 1998.

[3] P. Valente for the KLOE Drift Chamber Group, *The Construction of the KLOE Drift Chamber: Present Status*, in *Nucl. Instr. & Meth* **A409**, 87 (1998).

[4] G. Bencivenni, L. Bucci, G. Finocchiaro, C. Forti, P. Valente *Creep measurement on aluminum-5056 wires*, KLOE memo 138, 1997.

[5] G. Bencivenni *et al.*, *Sags in the KLOE Drift chamber*, KLOE memo, 1997.

[6] G. Bencivenni, P. Campana, G. Finocchiaro, P. Valente *A study on the crimping system of the KLOE Drift Chamber*, KLOE memo 136, 1997.

[7] The KLOE Drift Chamber Group, *Electrostatic digital method of wire tension measurement for the KLOE Drift Chamber*, in *Nucl. Instr. & Meth* **A409**, 63 (1998).

[8] G. Bencivenni, G. Finocchiaro, V. Golovatyuk, F. Grancagnolo, P. Valente, *Replacement of broken wires in the KLOE Drift Chamber*, KLOE memo 133, 1997.